TÜBİTAK

Turkish Journal of Chemistry

http://journals.tubitak.gov.tr/chem/

Research Article

Turk J Chem
(2019) 43: 568 – 581
© TÜBİTAK
doi:10.3906/kim-1808-78

Organotemplate-free Cs-ABW nanozeolite as highly reactive and recyclable catalyst for Henry reaction between benzaldehyde and nitroethane

Tamara Mahmoud ALI GHREAR[1], Ka-Lun WONG[2,3], Soon Huat TAN[4], Tau Chuan LING[5], Hussein AWALA[6], Eng-Poh NG[1,*]

[1]School of Chemical Sciences, Universiti Sains Malaysia, Penang, Malaysia
[2]School of Energy and Chemical Engineering, Xiamen University Malaysia, Sepang, Selangor, Malaysia
[3]College of Chemistry and Chemical Engineering, Xiamen University, Xiamen, P.R. China
[4]School of Chemical Engineering, Engineering Campus, Universiti Sains Malaysia, Penang, Malaysia
[5]Institute of Biological Sciences, Faculty of Science, University of Malaya, Kuala Lumpur, Malaysia
[6]Faculty of Sciences V, Lebanese University, Jdeidet, Lebanon

Received: 30.08.2018 • **Accepted/Published Online:** 31.12.2018 • **Final Version:** 03.04.2019

Abstract: Zeolite Cs-ABW nanocatalyst has been hydrothermally synthesized without using any harmful organic template. The zeolite nanocrystal with very high solid yield (81.88%) can be obtained within 60 min and at 180 °C (~20 atm), conditions that are much faster and gentler than the existing synthesis methods. The orthorhombic Cs-ABW nanocrystals (mean size of 32 nm) have high aluminum content (Si/Al ratio = 1.14) and possess high basicity. The nanocrystals also exhibit better catalytic activity than conventional homogeneous catalysts in the Henry (nitroaldol) reaction of benzaldehyde with nitroethane under microwave heating conditions. The nanocatalyst does not suffer from coking and leaching problems. It can be reused without loss of reactivity even after five consecutive runs under the described reaction conditions.

Key words: Cs-ABW nanozeolite, template-free hydrothermal synthesis, solid base catalyst, Henry reaction, microwave heating

1. Introduction

The Henry or nitroaldol reaction is one of the famous coupling reactions in organic chemistry to incorporate an alkylnitro group into a carbonyl compound.[1] It is a versatile reaction for synthesizing a variety of useful fine chemicals and pharmaceutical intermediates.[2] Essentially, the Henry reaction is made possible only in the presence of a base catalyst. Homogeneous catalysts such as NaOH, KOH, Na_2CO_3, pyridine, and amines are known to display unique catalytic performances in various reactions.[3] However, they suffer from several drawbacks such as low catalyst recovery, high disposal toxic waste, and low reaction selectivity.[4]

Zeolites are crystalline microporous aluminosilicates that have been widely used for adsorption, ion exchange, and catalysis.[5,6] Currently, more than 230 types of zeolites are known, but only some of them are commercially available and used in industry. ABW-type zeolite is a small-pore zeolite, where its 8 ring pores are organized in a zig-zag arrangement, forming a one-dimensional channel system (diameter of 3.4 × 3.8 Å^2).[7] Zeolites containing Cs^+ cations are of great interest due to their highly basic character that is appreciated in heterogeneous catalysis. The synthesis of zeolite Cs-ABW was reported in the 1970s but it requires extremely

*Correspondence: epng@usm.my

high temperature (700–1200 ?C) and pressure (>1000 bar).[8,9] Very recently, we successfully studied the nucleation and crystal growth of Cs-ABW zeolite nanocrystals in an organic-template-free hydrosol system using microscopy and spectroscopy techniques.[10] However, the properties of nanosized Cs-ABW zeolite are still not well understood, and hence an attempt to study the properties of these challenging zeolite nanocrystals is worthy of academic pursuit.

In the present study, nanosized Cs-ABW zeolite is crystallized under rapid and safer hydrothermal conditions using an organotemplate-free system. Characterization and catalytic performance of the synthesized Cs-ABW in the Henry reaction of benzaldehyde with nitroethane are then reported.

2. Results and discussion

2.1. Synthesis of Cs-ABW zeolite nanocrystals

Nanocrystalline Cs-ABW zeolite has been synthesized via hydrothermal treatment at 180 ?C. The HT-10m solid was amorphous according to X-ray diffraction (XRD) results (Figure 1a). When the heating time was extended to 60 min, the ABW crystalline phase was obtained as the solid exhibited major diffraction peaks at 2θ = 18.80°, 26.94°, 27.52°, 32.90°, and 38.78°, which were attributed to the (200)/(110), (211), (202)/(112), (310)/(020), and (312)/(022) planes of the ABW-type zeolite, respectively (Figure 1b).[7] The diffraction peaks were broad and intense, indicating small crystallite size and high crystallinity of the nanocrystals.

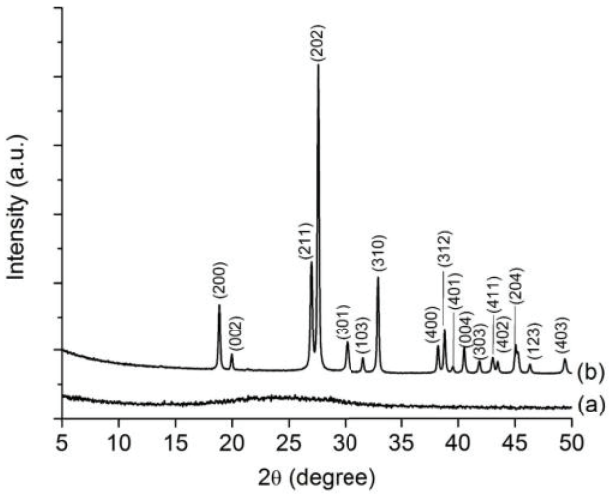

Figure 1. XRD patterns of (a) HT-10m (amorphous) and (b) HT-60m (zeolite Cs-ABW).

The morphology of HT-10m and HT-60m was studied using transmission electron microscopy (TEM). Amorphous HT-10m nanoparticles (ca. 18 nm) displayed no apparent shape while crystalline HT-60m exhibited discrete nanoparticles (ca. 27 nm) with some crystals having an orthorhombic shape with rounded corners, which was different from that of Li-ABW micron-sized crystals (Figures 2a–2d).[11,12] Meanwhile, field-emission scanning electron microscopy (FESEM) images also revealed that the nanocrystals did not agglomerate and they had very narrow particle size distribution, sizing from 18 nm to 59 nm with a mean crystal size of 32.3 nm (Figures 2e and 2f).

The N_2 sorption analysis of HT-60m displayed a type IV isotherm with type H1 hysteresis loop showing the characteristic of interparticle mesoporosity (Figure 3a).[13] The nanocrystals had a total BET surface area

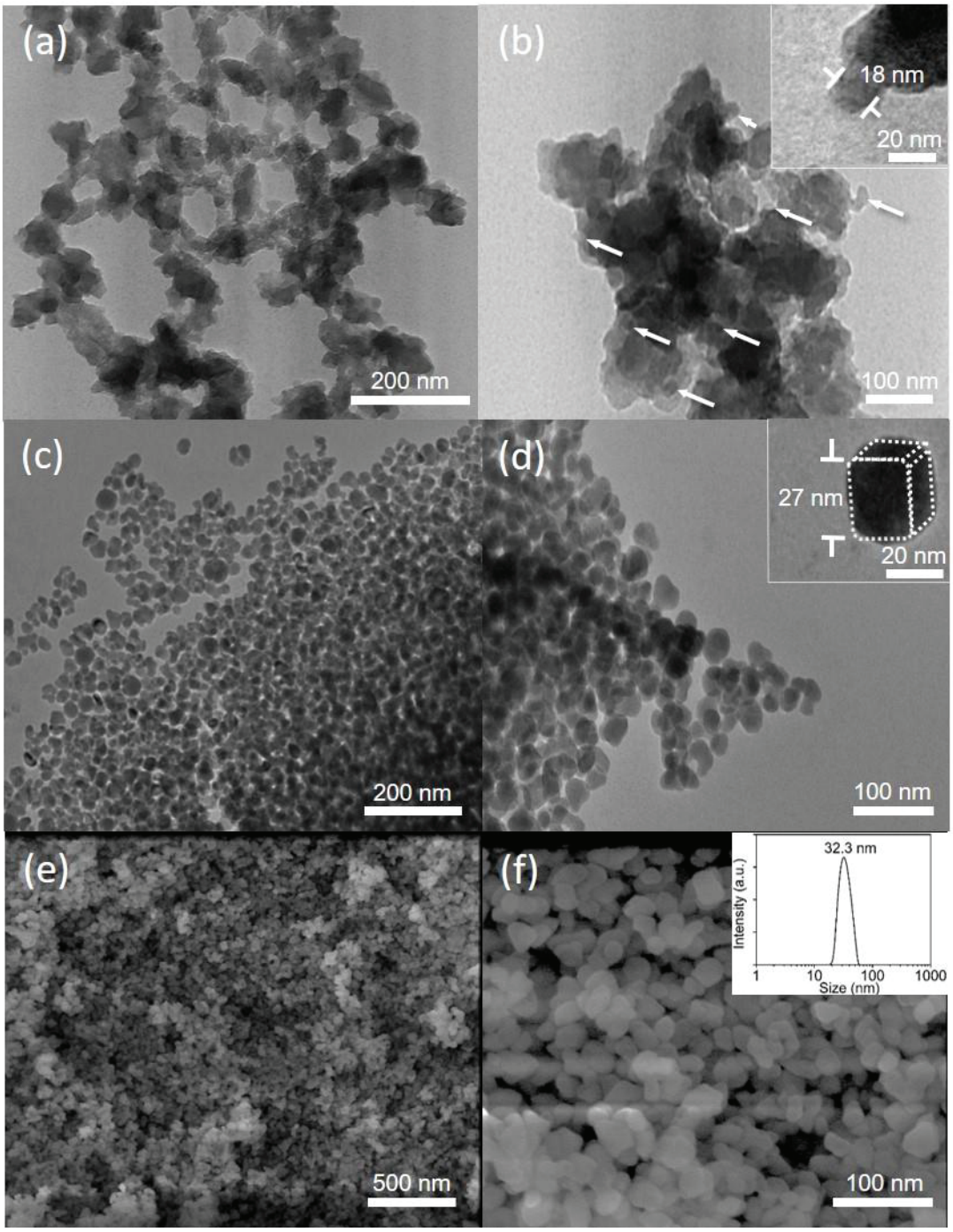

Figure 2. TEM images of (a,b) HT-10m and (c,d) HT-60m (zeolite Cs-ABW), and (e,f) SEM images of HT-60m at different magnifications. Inset of (f): particle size distribution of HT-60m.

of 119 m^2/g and total pore volume of 0.463 cm^3/g. Low micropore surface area (10 m^2/g) was measured due to the small pores of the ABW zeolite framework that disallowed the diffusion of N_2 molecules.[14] As a result, most of the surface area of the Cs-ABW nanocrystals measured was contributed by their external/mesopore surface (109 m^2/g). The pore size distribution of HT-60m was from 28 nm to 550 nm, centered at 156.1 nm

according to the BJH model (inset of Figure 3a). Such large pore opening is highly demanded in heterogeneous catalysis since it promotes fast diffusion and accessibility.

The functional groups of nanosized Cs-ABW zeolite were characterized with IR spectroscopy. The IR bands at 3465 and 1665 cm^{-1} were due to the O-H stretching and bending vibrations of the adsorbed water, respectively (Figure 3b).[15] The IR bands at 986 and 1130 cm^{-1} were assigned to the internal vibrations of Si–O–T (T = Si, Al) asymmetric stretching modes, while the signal at 1062 cm^{-1} was attributed to the Si–O–T symmetric stretching vibration mode.[16] Several weak signals observed at 541, 608, and 671 cm^{-1} were characteristic of the double zigzag chain present in the ABW framework structure.[17] The small peak that resonated at 882 cm^{-1} was due to the presence of the TO–H group and a weak band at 449 cm^{-1} corresponded to the bending vibration of TO_4.

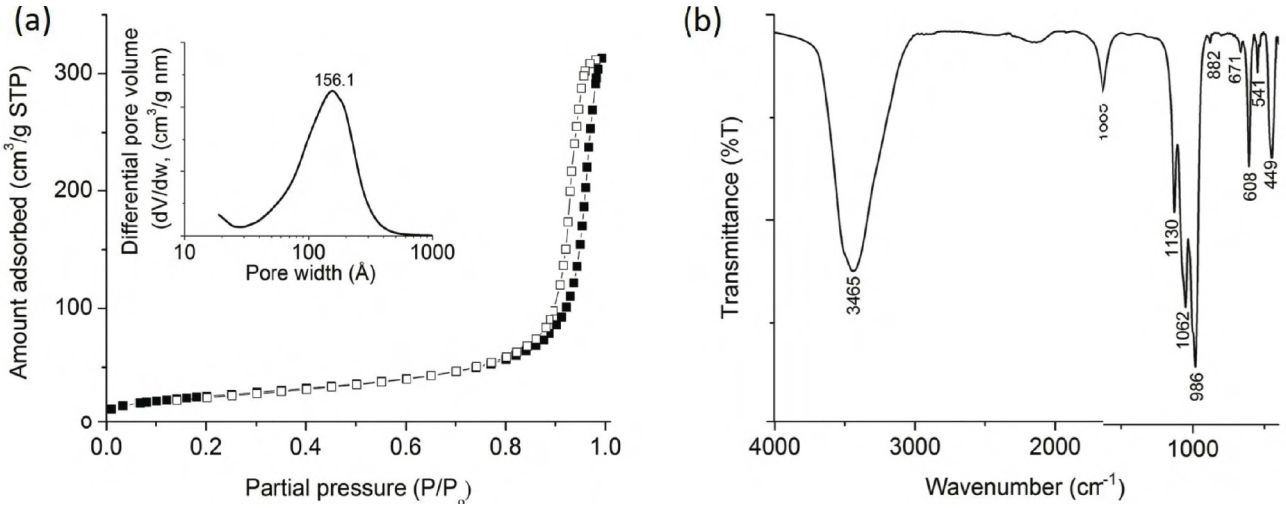

Figure 3. (a) Nitrogen adsorption (closed symbols) and desorption (open symbols) isotherms, and (b) IR spectrum of HT-60m (zeolite Cs-ABW). Inset of (a): pore size distribution of HT-60m.

EDX analysis with elemental mapping study was performed on nanosized ABW zeolite (HT-60m) (Figure 4). As shown, Al, Si, Cs, and O elements were abundant and evenly distributed in all granules. The quantitative EDX analysis results shown in Table 1 indicated that the Si/Al ratio was 1.14 while the Cs/Al ratio was 0.99, which is close to unity. Thus, the elemental analysis revealed that the nanosized Cs-ABW zeolite might have basicity where its basic sites originate from the framework oxygen atoms, $(Si–\mathbf{O}–Al)^- Cs^+$.[18]

Table 1. EDX chemical analysis of HT-60m (zeolite Cs-ABW).

Sample	Elements (wt.%)					Molar ratios	
	O	Al	Si	Cs	Total	Si/Al	Cs/Al
HT-60m	36.06	9.05	10.69	44.20	100.00	1.14	0.99

The above hypothesis was confirmed by temperature-programmed desorption of carbon dioxide (CO_2-TPD) analysis (Figure 5). Three CO_2 desorption peaks were obtained after deconvolution. The first peak at 83 °C was from the interaction between CO_2 and the weak basic sites at the external surface of the nanocrystals.[19] The peaks centered at 472 °C and 646 °C originated from the medium and strong basic sites located at the

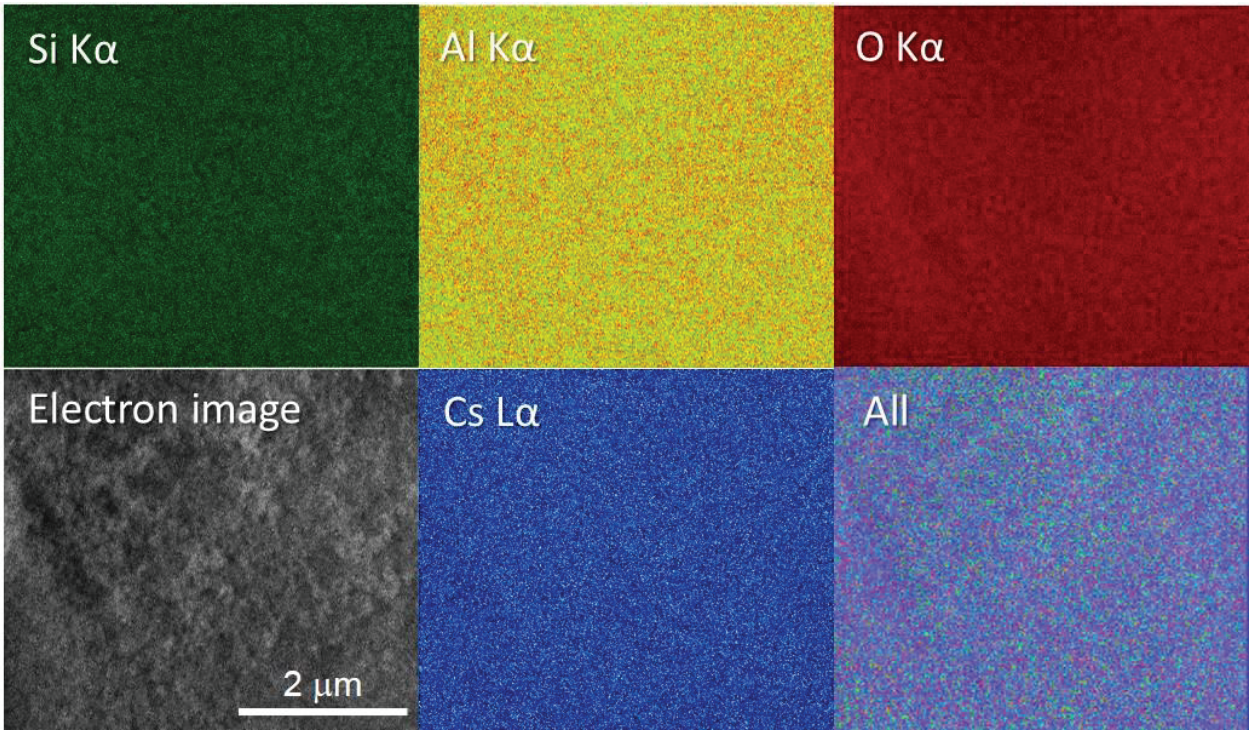

Figure 4. Element distribution map (SEM/EDX) of HT-60m (zeolite Cs-ABW).

textural pores of the solid.[20] Both CO_2 desorption peaks were considerably intense due to the highly accessible textural mesopores.

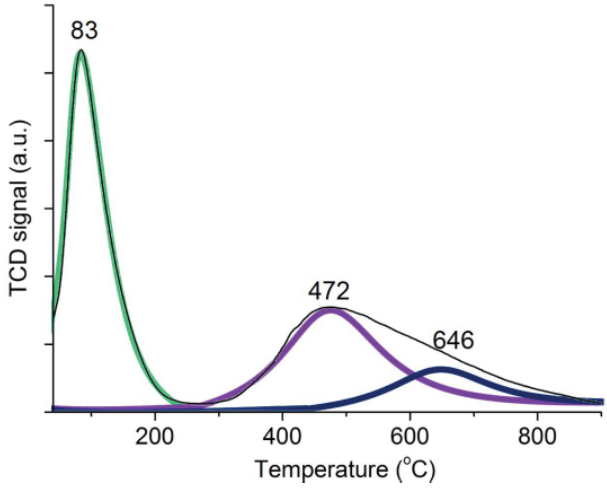

Figure 5. TPD-CO_2 plot of HT-60m (zeolite Cs-ABW) with deconvolution curves.

2.2. Catalytic Henry reaction between benzaldehyde and nitroethane

Microwave-assisted nitroaldol reaction between benzaldehyde and nitroethane was chosen as a model reaction (Eq. (1)) to study the potential of nanosized Cs-ABW zeolite as a solid base catalyst. The effects of reaction

time, temperature, catalyst loading, benzaldehyde to nitroethane molar ratio, solvent, and heating mode were studied. Furthermore, catalyst comparative study and catalyst reusability testing were also investigated.

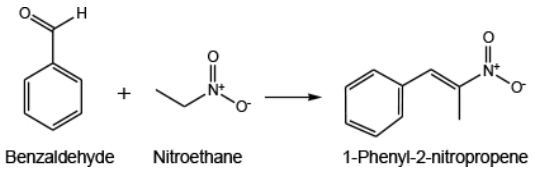

(1)

2.2.1. Effect of reaction temperature and time

The catalytic activity of nanosized ABW zeolite (HT-60m) in nitroaldol reaction between benzaldehyde and nitroethane was studied at different temperatures for 70 min of microwave irradiation (Figure 6). At 160 °C, significant color change was observed when the reaction was taking place (Figure 6a). The transparent color reactant initially changed to pale yellow (10 min), yellow (20 min), orange (30 min), and brown (40 min) before a dark brown solution was obtained after 70 min of reaction. These reaction solutions were further characterized with GC. At 160 °C, 89.2% of conversion with 100% selectivity to the desired product was achieved (Figure 6b, line a). The reaction was also carried out at 130 °C, 140 °C, and 150 °C (Figure 6b, lines b–d). The reaction conversion rate decreased while lowering the reaction temperature, while the selectivity of the targeted phenyl-2-nitropropene remained constant. The amount of nonreacted benzaldehyde at different times under microwave heating at 160 ?C was recorded in order to determine the reaction order. The reaction was found to follow second-order reaction kinetics with $k_{with\ catalyst,\ 160\,^{\circ}C} = 0.4531\ min^{-1}$. In the absence of nanosized Cs-ABW zeolite catalyst, the nitroaldol reaction still took place ($k_{without\ catalyst,\ 160\,^{\circ}C} = 0.0233\ min^{-1}$), but with a much lower conversion rate (27.8%). This is due to the fact that introducing a solid catalyst in the reaction system increases the tendency of molecular contact between reactants via adsorption and will therefore increase the reaction rate.[21]

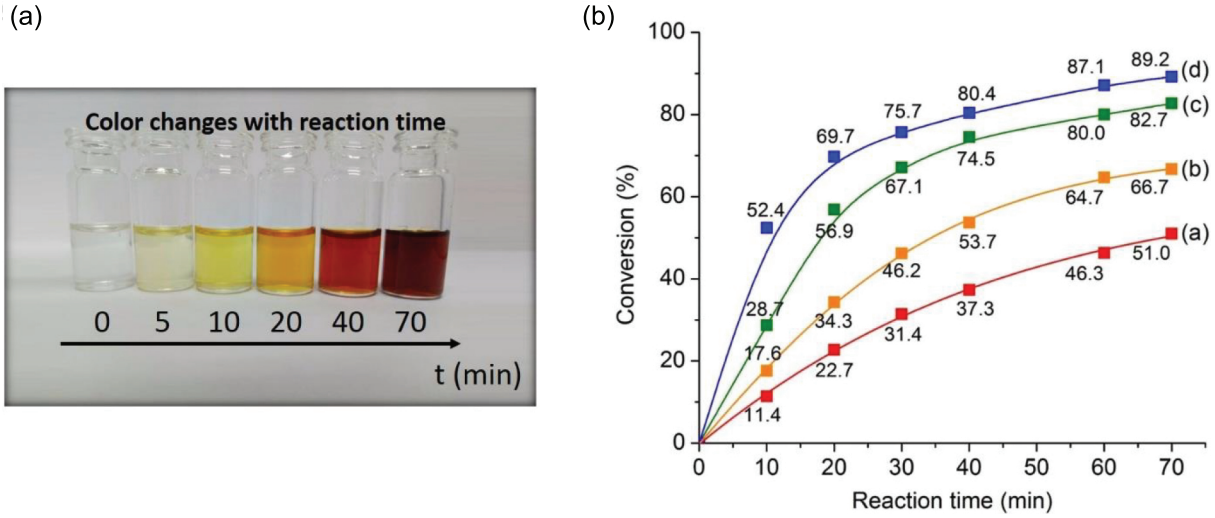

Figure 6. (a) Appearance of reaction solution after subsequent reaction times and (b) effect of temperature on the conversion at a- 130 °C, b- 140 °C, c- 150 °C, and d- 160 °C. Catalyst (HT-60m) = 0.50 g, benzaldehyde = 2 mmol, nitroethane = 40 mmol, solvent-free.

The activation energy (E_a) of both the catalyzed and noncatalyzed reactions was calculated by using the Arrhenius equation in order to further understand the reaction kinetics of the catalytic reactions. The rate constants were obtained at 130 ?C, 140 ?C, 150 ?C, and 160 ?C and ln k versus 1/T was plotted. The E_a of nitroaldol reaction with the presence of nanosized Cs-ABW zeolite was 101.4 kJ mol^{-1}, which was much lower than that without catalyst (179.0 kJ mol^{-1}). Hence, this shows that nitroaldol reaction is an activated catalytic reaction where nanosized Cs-ABW zeolite provides an alternate pathway for the reaction that has lower activation energy.[22] From this study, the optimum temperature and reaction time were chosen to be 160 °C and 60 min for further catalytic study.

2.2.2. Effect of catalyst loading

The effect of catalyst loading was studied in the range of 0–0.75 g using the following conditions: 160 °C, 60 min, benzaldehyde : nitroethane molar ratio = 2 mmol : 40 mmol. Only 17.7% conversion was observed when no catalyst was applied (Figure 7). The conversion rate increased significantly when more Cs-ABW nanocatalyst was added. The highest conversion rate of 87.1% was achieved with 0.50 g of catalyst. Nevertheless, further increasing the catalyst amount to 0.75 g resulted in a decrease in the conversion to 75.6% but the selectivity to the desired product remained 100%. This phenomenon could be explained by the fact that the solid particles tend to come closer and agglomerate when a high loading of solid catalyst is used. As a result, it makes stirring more difficult and less efficient. Thus, lower conversion is expected when an overdose of catalyst is used. From this study, 0.50 g of Cs-ABW nanocatalyst was chosen for the further catalytic study.

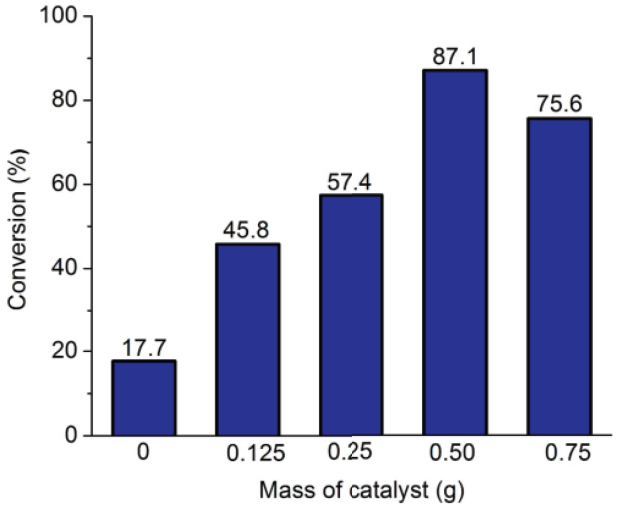

Figure 7. Percentage of conversion of benzaldehyde of Henry reaction at different amounts of catalyst (HT-60m). Reaction temperature = 160 °C, time = 60 min, benzaldehyde = 2 mmol, nitroethane = 40 mmol, solvent-free.

2.2.3. Effect of benzaldehyde to nitroethane molar ratio

The effect of benzaldehyde to nitroethane molar ratio was studied while the other reaction parameters were kept constant (Figure 8). In general, the selectivity towards the targeted product was not affected by adjusting the reactant ratios. The conversion was 63.5% when the benzaldehyde to nitroethane molar ratio was 2:10. The highest conversion, 87.10%, was achieved when the ratio was increased to 2:40. However, the catalytic conversion

started to decrease with further increasing of the nitroethane concentration. The nitroaldol Henry reaction was also performed with nitroethane as a limiting reagent. Interestingly, a very low conversion (15%–11%) was observed when the benzaldehyde to nitroethane molar ratio was adjusted to 50:2 and 40:2. The results thus revealed that nitroethane has to be activated first on the catalyst surface before reacting with benzaldehyde.[23] Based on the results obtained, the benzaldehyde to nitroethane molar ratio of 2:40 was used for further catalytic studies.

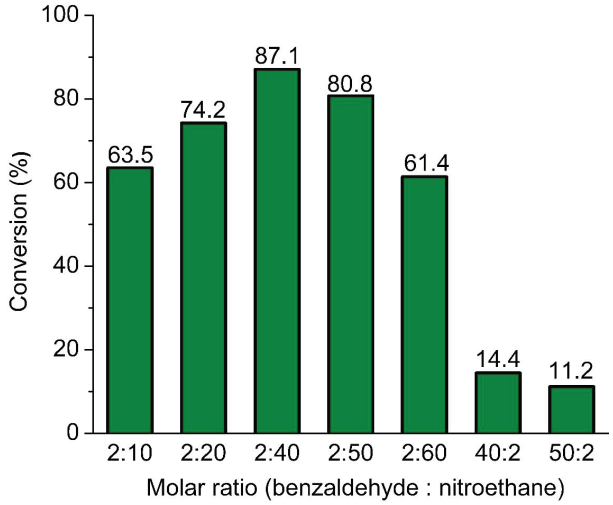

Figure 8. Percentage of conversion of benzaldehyde at different benzaldehyde : nitroethane molar ratios. Reaction temperature = 160 °C, time = 60 min, catalyst (HT-60m) = 0.50 g.

2.2.4. Effects of solvent

Solvents play an important role in catalytic reactions due to their specific properties (e.g., polarity, hydrophilicity, microwave dielectric heating).[24] Hence, five solvents (dichloromethane, acetonitrile, dimethyl sulfoxide, n-heptane, and water) with different empirical solvent polarities (E_T^N scale) and microwave absorptivities (tan δ) were chosen in this study.[25,26] In general, the results showed that the reaction conversion followed the trend of solvent polarity instead of the microwave loss factor while the selectivity to the targeted 1-phenyl-2-nitropropene was still 100% (Table 2). For instance, the reactions run with dimethyl sulfoxide and acetonitrile polar solvents gave higher product conversion (>95.0%) than those run with dichloromethane and n-heptane solvents. Nevertheless, the catalytic performance was poor when water, another very polar solvent (E_T^N = 1.00), was used. This could be explained by the tendency of water for poisoning the basic sites of the Cs-ABW nanocatalyst.[27] Another possibility is the inability of water to dissolve benzaldehyde and nitroethane (organic reactants), hence leading to inefficient mass and heat transfers during diffusion, adsorption, and reaction processes.

2.2.5. Catalyst comparative study

Catalyst comparative study was performed in the microwave-assisted nitroaldol condensation reaction where KOH, $NaHCO_3$, NaOH, K_2CO_3, CsOH, and Cs-ABW zeolite nanocatalyst were tested (Figure 9). Excitingly, the nanosized Cs-ABW zeolite showed the best catalytic performance (87.1% conversion), followed by KOH (56.4% conversion), K_2CO_3 (52.3% conversion), NaOH (33.2%), and $NaHCO_3$ (32.0% conversion) where all

Table 2. Effect of solvent on nitroaldol condensation reaction.[a]

Solvents	Polarity in E_T^N scale	Microwave loss factor (tan δ)	Conversion (%)
Dimethyl sulfoxide	0.444	0.825	98.2
Acetonitrile	0.460	0.062	96.4
n-Heptane	0.012	0.020	92.4
Dichloromethane	0.309	0.042	86.3
Water	1.00	0.123	30.1
Solvent-free	-	-	87.1

[a]Reaction conditions: temperature = 160 °C, time = 60 min, benzaldehyde = 2 mmol, nitroethane = 40 mmol, solvent volume = 4 mL, catalyst (HT-60m) = 0.50 g.

catalysts only yielded 1-phenyl-2-nitropropene. The high reaction conversion could be explained by the basicity strength of the catalyst, which is a crucial factor to activate nitroethane. On the other hand, CsOH exhibited very high catalytic activity in this reaction under similar reaction conditions (98.1% conversion), but product decomposition was also observed with only 42.2% selectivity to phenyl-2-nitropropene. Nevertheless, the CsOH homogeneous catalyst achieved comparable catalytic performance as Cs-ABW nanocatalyst at 140 °C after 60 min of microwave heating (85.3% conversion, 100% selective to phenyl-2-nitropropene).

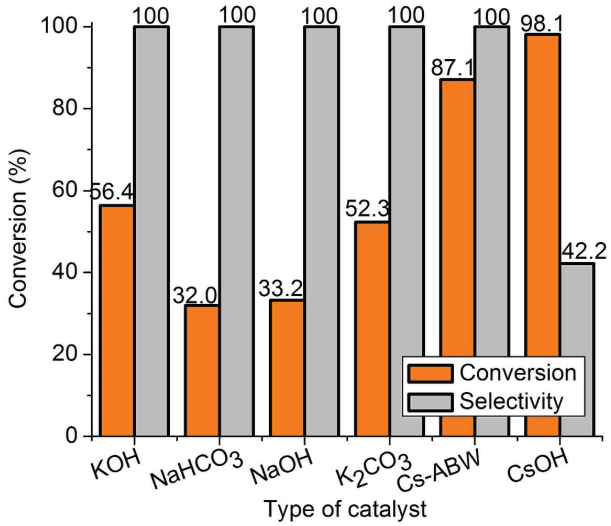

Figure 9. Percentage of conversion of benzaldehyde using different types of catalyst (1.984 mmol equivalent to 0.50 g ABW nanocatalyst). Reaction temperature = 160 °C, time = 60 min, benzaldehyde = 2 mmol, nitroethane = 40 mmol, solvent-free.

The catalytic performance of nanosized Cs-ABW zeolite for the Henry reaction was also compared with those reported using homogeneous catalysts (Table 3). It was shown that microwave-assisted Henry reaction using nanosized Cs-ABW zeolite catalyst exhibited much higher conversion (87.1%) than those using homogeneous base catalysts (NH_4OAc, *n*-$BuNH_2$, organotin complexes)[28,29] heated under reflux while all catalysts gave 100% selectivity towards 1-phenyl-2-nitropropene.

Table 3. Comparison of nanosized Cs-ABW zeolite catalyst with reported homogeneous catalyst systems.

Catalyst	Conversion (%)	Selectivity (%)	Time (h)	Heating mode	Reference
Nanosized Cs-ABW	87.1	100	1	Microwave	This work
NH_4OAc	59	100	4	Reflux	[28]
n-$BuNH_2$	71	100	8	Reflux	[28]
Organotin(IV) complexes	78	100	6	Reflux	[29]

2.2.6. Effect of reaction mode

Three different reaction modes were tested in this investigation, namely conventional reflux, autoclave, and microwave heating, where the following conditions were used: 160 °C, benzaldehyde = 2 mmol, nitroethane = 40 mmol, catalyst (HT-60m) = 0.50 g, solvent-free. As predicted, conventional reflux, which involved conduction heating and a noneffective heat transfer mechanism, required a very long reaction time (24 h) to achieve merely 26.0% reaction conversion. On the other hand, autoclave mode took just 12 h to achieve higher conversion (54.3%) thanks to the autogenic pressure exerted at high temperature (160 °C). As a comparison, 87.1% of product conversion could be achieved within 1 h with microwave reaction mode while the product selectivity is maintained as high as 100%. Therefore, the microwave mode significantly enhanced the nitroaldol condensation reaction by providing efficient and uniform molecular level heating.[30] In addition, under electromagnetic microwave radiation, the reactant molecules are also rotationally excited, leading to more reactant collisions that provoke chemical reactions and thus resulting in higher conversion.[31]

2.2.7. Catalyst reusability test

Solid catalysts always suffer from reusability problems.[32] Therefore, a reusability test for nanosized Cs-ABW zeolite was performed (Figure 10a). The reactivity of the recycled nanocatalyst was preserved for at least up to five reaction cycles. The results suggested that the Cs^+ cations are electrostatically and strongly bound to the surface of the nanosized zeolite.[33] The coke content of nanosized Cs-ABW zeolite was determined by TGA/DTG analysis (Figure 10b). Interestingly, no significant weight loss was observed above 200 ?C. This indicated that the catalyst did not suffer from coking problem due to its easy accessible external surface. This observation was further supported by N_2 adsorption-desorption isotherm and TEM analyses where the surface area and the morphology of the solid were not significantly affected (Figures 10c and 10d).

2.3. Conclusion

Nanosized Cs-ABW zeolite has been successfully synthesized free of organic template using a conventional hydrothermal method (180 ?C, ~20 atm, 60 min). The nanocrystals with orthorhombic morphology (~32 nm) possess high textural mesoporosity and high basicity character. It has been proven as an excellent and recyclable solid base catalyst in the Henry nitroaldol reaction of benzaldehyde with nitroethane. This nanocrystalline material with accessible mesoporosity and high basicity has great potential in advanced applications, particularly in film deposition and catalytic technologies.

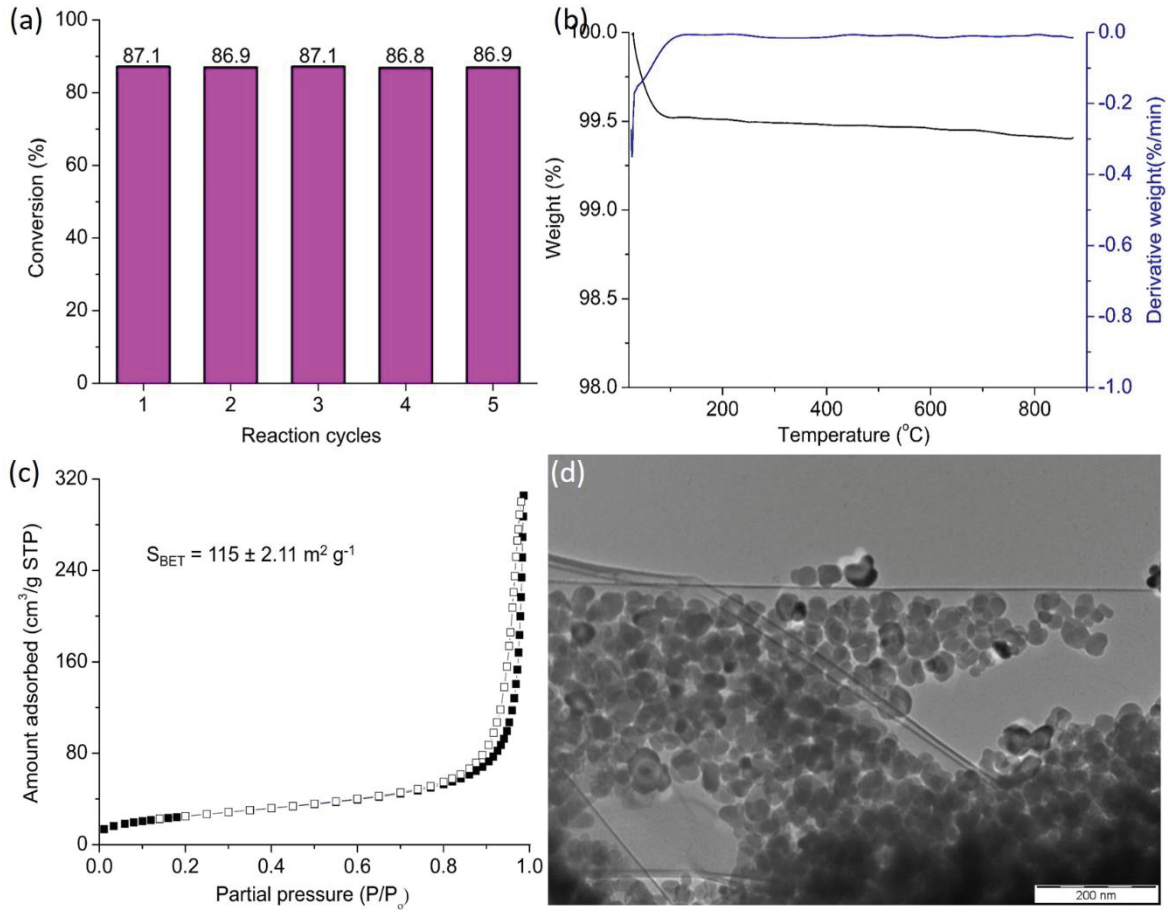

Figure 10. (a) Catalyst reusability test, (b) TGA/DTG profiles, (c) nitrogen gas sorption isotherm plot, and (d) TEM image of HT-60m (nanosized zeolite Cs-ABW) after catalytic reaction.

3. Experimental

3.1. Synthesis of Cs-ABW zeolite nanocrystals

The nanosized Cs-ABW zeolite was prepared by first preparing two solutions, namely aluminate (A) and silicate (B) solutions. Solution A was prepared by mixing $CsOH \bullet H_2O$ (3.500 g, $\geq$99.5%, Sigma-Aldrich), $Al(OH)_3$ (0.414 g, extra pure powder, Acros), and distilled water (2.688 g) in a 125-mL polypropylene bottle. The mixture was heated at 105 °C for 16 h under continuous stirring (380 rpm) to obtain a clear solution. Solution B was prepared by dissolving HS-40 (1.594 g, Sigma-Aldrich) and $CsOH \bullet H_2O$ (10.763 g) in distilled water (2.663 g). Both solutions were allowed to cool to room temperature before solution A was added slowly to solution B under vigorous stirring (15 min). The resulting clear precursor hydrosol with a molar composition of $4SiO_2$:$1Al_2O_3$:$16Cs_2O$:$164H_2O$ was then transferred to a Teflon-lined stainless steel autoclave before being heated at 180 °C for 60 min. The synthesis was repeated by changing the heating time to 5 and 10 min, respectively. The resulting white colloidal suspensions were centrifuged (10,000 rpm, 7 min) and purified with distilled water until pH 7–8. Finally, the white colloid solutions were freeze-dried. The samples were denoted as HT-nm, where n is the hydrothermal heating time.

3.2. Characterization

The crystalline phase and purity of the solid products were studied by powder XRD (Siemens D500 diffractometer, CuK_α radiation, $\lambda = 1.5406$ Å, scan speed of 0.2°/min, step size of 0.02°). The crystal size and morphology of the sample were measured by a Philips CM12 TEM and JEOL JSM- 6701F FESEM operated at 200 kV and 20 kV, respectively. The formation of the structural framework of zeolite was studied with a PerkinElmer FTIR spectrometer (System 2000) in the range of 400–1400 cm^{-1}. KBr pellet technique (KBr:sample ratio = 50:1) was used to prepare the transparent pellets. The chemical composition and elemental mapping of the sample were determined by using a JEOL JSM- 6701F FESEM equipped with an Oxford Instruments X-Max 80 mm^2 Solid State EDX detector. The porosity measurement of the solid sample was performed using a Micromeritics ASAP 2010 nitrogen adsorption analyzer. The sample was degassed at 300 °C under vacuum overnight prior to sorption at –196 °C. The basic strength of the zeolite was studied via CO_2-TPD using a BELCAT-B apparatus, which was connected to a thermal conductivity detector. First, the powder sample (ca. 80 mg) was degassed at 300 °C overnight and adsorbed with CO_2 gas, followed by slow desorption in the temperature range of 40 to 900 °C at a heating rate of 10 °C/min. TGA/DTG analysis was carried out by using a Mettler TGASDTA851 instrument with a heating rate of 20 °C min^{-1} under air flow. The results collected were recorded as percent weight loss (wt.%) versus temperature (?C).

3.3. Catalytic activity study

The Henry (nitroaldol) reaction of benzaldehyde with nitroethane was performed as follows: activated Cs-ABW (0.50 g, 300 °C, 3 h), nitroethane (40 mmol, 97% Merck), and benzaldehyde (2 mmol, 99% Merck) were loaded into a 10-mL quartz vial. The vial was tightly capped and irradiated with microwaves (850 °C output power, Monowave 300) at a desired temperature for a specific time. After the process was complete, the reaction solution was separated from the solid catalyst using centrifugation (10,000 rpm, 8 min). The reaction product was injected into a GC-FID (Agilent 7890A) and a GC-MS (Agilent 7000 Series Triple Quad GC/MS) equipped with a DB-5 capillary column for chromatography analysis. Toluene was used as an internal standard. The conversion and the selectivity of the reaction were calculated by using the following equations:

$$\text{Conversion } (\%) = 100 - [(A_{Benzaldehyde}/A_{Toluene})t_i \times (A_{Toluene}/A_{Benzaldehyde})t_0 \times 100] \quad (2)$$

$$\text{Selectivity } (\%) = (A_{Phenyl-2-nitropropene}/A_{Benzaldehyde}) \times 100 \quad (3)$$

Here, $A_{Benzaldehyde}$ is the peak area of benzaldehyde, $A_{Toluene}$ is the peak area of toluene, t_0 is the reaction at time 0 h, t_i is the reaction at time i h, and $A_{Phenyl-2-nitropropene}$ is the peak area of phenyl-2-nitropropene.

3.4. Reusability tests

Cs-ABW zeolite nanocrystals, which were used for the first reaction run, were washed with diethyl ether (15 mL, 5 times), air-dried, and reactivated before being used for the next cycles of catalytic reaction under the previous experimental conditions. After the reaction was completed, the solution was separated from the zeolite catalyst and analyzed using a GC-FID.

Acknowledgment

The financial support from RUI (1001/PKIMIA/8011012) and SATU Joint Research Scheme (RU018O-2016), is acknowledged.

References

1. Cheng, L.; Dong, J.; You, J.; Gao, G.; Lan, J. *Chem. Eur. J.* **2010**, *16*, 6761-6765.
2. Ballini, R.; Bosica, G. *J. Org. Chem.* **1997**, *62*, 425-427.
3. Clarina, T.; Valentina, B. M.; Rama, V. *Int. J. Sci. Res.* **2014**, *3*, 2399-2403.
4. Lima, A. L. D.; Ronconi, C. M.; Mota, C. J. A. *Catal. Sci. Technol.* **2016**, *6*, 2877-2891.
5. Davis, M. E. *Nature* **2002**, *417*, 81.
6. Rahimi, M.; Ng, E. P.; Bakhtiari, K.; Vinciguerra, M.; Ahmad, H. A.; Awala, H.; Mintova, S.; Daghighi, M.; Rostami, F. B.; de Vries, M. et al. *Sci. Rep.* **2015**, *5*, 17259.
7. Baerlocher, C.; McCusker, L. B.; Olson, D. H. *Atlas of Zeolite Framework Types*; Elsevier: Amsterdam, the Netherlands, 2007.
8. Klaska, R.; Jarchow, O. *Naturwissenschaften* **1973**, *60*, 299.
9. Klaska, R.; Jarchow, O. *Z. Kristallogr.* **1975**, *142*, 225-238.
10. Ghrear, T. M. A.; Rigolet, S.; Daou, T. J.; Mintova, S.; Ling, T. C.; Tan, S. H.; Ng, E. P. *Micropor. Mesopor. Mater.* **2019**, *277*, 78-83.
11. Liu, H. G.; Shi, Q.; Liu, L.; Xu, H.; Li, J.; Dong, J. *Stud. Surf. Sci. Catal.* **2008**, *174A*, 185-188.
12. Spektor, K.; Fischer, A.; Haussermann, U. *Inorg. Chem.* **2016**, *55*, 8048-8058.
13. Ng, E. P.; Ling, J. Y; Ling, T. C.; Mukti, R. R. *Nanoscale Res. Lett.* **2013**, *8*, 120.
14. Cheong, Y. W.; Wong, K. L.; Ling, T. C.; Ng, E. P. *Mater. Exp.* **2018**, *8*, 463-468.
15. Ng, E. P.; Ng, D. T. L.; Awala, H.; Wong, K. L.; Mintova, S. *Mater. Lett.* **2014**, *132*, 126-129.
16. Wong, S. F.; Awala, H.; Vincente, A.; Retoux, R.; Ling, T. C.; Mintova, S.; Mukti, R. R.; Ng, E. P. *Micropor. Mesopor. Mater.* **2017**, *249*, 105-110.
17. Norby, P.; Christensen, A. N.; Andersen, I. G. K. *Acta Chem. Scand.* **1986**, *A40*, 500.
18. Mignon, P.; Geerlings, P.; Schoonheydt, R. *J. Phys. Chem. B* **2006**, *110*, 24947-24954.
19. Wong, S. F.; Deekamwong, K.; Wittakayun, J.; Ling, T. C.; Muzara, O.; Lee, H. L.; Adam, F.; Ng, E. P. *Sains Malays.* **2018**, *47*, 337-345.
20. Saceda, J. J. F.; Leon, R.; Rintramee, K.; Prayoonpokarach, S.; Wittayakun, J. *Quim. Nova* **2011**, *34*, 1394-1397.
21. Hemalatha, K.; Madhumitha, G.; Kajbafvala, A.; Anupama, N.; Sompalle, R.; Roopan, S. M. *J. Nanomater.* **2013**, *2013*, 1-23.
22. Ng, E. P.; Lim, G. K.; Khoo, G. L.; Tan, K. H.; Ooi, B. S.; Adam, F.; Ling, T. C.; Wong, K. L. *Mater. Chem. Phys.* **2015**, *155*, 30-35.
23. Luzzio, F. A. *Tetrahedron* **2001**, *57*, 915-945.
24. Li, C. J.; Trost, B. M. *P. Natl. Acad. Sci. USA* **2008**, *105*, 13197-13202.
25. Zou, J.; Yu, Q.; Shang, Z. *J. Chem. Soc. Perkin Trans.* **2001**, *2*, 1439-1443.
26. Tompsett, G. A.; Conner, W. C.; Yngvesson, K. S. *ChemPhysChem* **2006**, *7*, 296-319.
27. Hattori, H. *Appl. Catal. A Gen.* **2015**, *504*, 103-109.
28. Andrighetto, L. M.; Henderson, L. C.; Pearson, J. R.; Stevenson, P. G.; Conlan, X. A. *Aust. J. Forensic Sci.* **2016**, *48*, 684-693.

29. Gurbanov, A. V.; da Silva, M. F. C. G.; Kustov, L. M.; Guseinov, F. I.; Mahmudov, K. T.; Pombeiro, A. J. L. *J. Organometal. Chem.* **2018**, *867*, 98-101.

30. Wong, S. F.; Deekomwong, K.; Wittayakun, J.; Ling, T. C.; Muraza, O.; Adam, F.; Ng, E. P. *Mater. Chem. Phys.* **2017**, *196*, 295-301.

31. Horikoshi, S.; Serpone, N. *Catal. Sci. Technol.* **2014**, *4*, 1197-1210.

32. Golmohamadpour, A.; Bahramian, B.; Shafiee, A.; Mamani, L. *Mater. Chem. Phys.* **2018**, *218*, 326-335.

33. Mohammad, A. G. S.; Ahmad, N. H.; Goldyn, K.; Mintova, S.; Ling, T. C.; Ng, E. P. *Mater. Res. Exp.* **2019**, *6*, 025026.